JOURNAL OF SOLID STATE CHEMISTRY 115, 152–157 (1995)

Chemical Diffusion in Polycrystalline Calcium-Doped Lanthanum Chromites

I. Yasuda[1] and M. Hishinuma

Fundamental Technology Research Laboratory, Tokyo Gas Co., Ltd., Shibaura, Minato-ku, Tokyo, 105 Japan

Received March 29, 1994; in revised form July 12, 1994; accepted July 15, 1994

The chemical diffusion coefficient of polycrystalline calcium-doped lanthanum chromites, $La_{1-x}Ca_xCrO_{3-\delta}$, was measured as a function of oxygen partial pressure, composition, and temperature by means of electrical conductivity relaxation. The measured chemical diffusivity increased with increasing oxygen vacancy concentration, the mechanism of which was discussed in light of defect chemical equilibrium. The derived vacancy diffusion coefficient was independent of the vacancy concentration, suggesting that oxygen vacancies were randomly distributed. © 1995 Academic Press, Inc.

1. INTRODUCTION

The chemical stability in both oxidizing and reducing atmospheres at elevated temperatures and the good electrical properties of perovskite-type oxides based on $LaCrO_3$ make them useful as high temperature electronic conductors, including interconnectors for solid oxide fuel cells (SOFCs). When used as an interconnector in the SOFC, the existence of a large oxygen chemical potential gradient makes knowing the oxygen diffusivity and understanding the diffusion mechanism important. Very few studies, however, have been concerned with oxygen diffusivity in lanthanum chromites. Yu *et al.* (1) measured the chemical diffusion coefficient of sintered ceramics of Mg-doped $LaCrO_3$ by means of the conductivity relaxation technique and concluded that its high diffusivity and low activation energy were attributable to grain boundary diffusion. Van Dieten *et al.* (2) attempted to evaluate ionic conductivity in dynamically compacted Mg-doped $LaCrO_3$ using semiblocking solid-state electrochemical cells where yttria-stabilized zirconia was employed as the solid electrolyte. They reported that it was difficult to definitely assign the impedance spectra to particular physical processes. The accumulation of data from various experimental techniques will be required to obtain the true oxygen diffusivity in $LaCrO_3$-based materials.

In this study, chemical relaxation experiments were conducted on sintered polycrystalline specimens of Ca-doped $LaCrO_3$, where an abrupt change in oxygen chemical potential in the surrounding atmosphere was imposed upon the sample and time change of electrical conductivity was recorded. Following our previous reports highlighting the details of experimental and analytical procedures (3, 4), this paper focuses on interpreting the results in light of defect chemical equilibrium.

2. EXPERIMENTAL

Raw material powders of three compositions, $x = 0.1$, 0.2, and 0.3 in $La_{1-x}Ca_xCrO_{3-\delta}$ (δ is the mole fraction of oxygen deficiency), were synthesized by a high-temperature solid-state reaction of mixtures of La_2O_3, $CaCO_3$, and Cr_2O_3 powders. Cylindrical samples of 4 to 5 mm diameter and 25 to 30 mm length were obtained by isostatically pressing the synthesized powder followed by sintering at 1450 to 1600°C in air. The density of the sintered samples was over 95% of the theoretical density, and the average grain size was about 5 μm from the SEM observations. XRD analyses confirmed the samples to be single phase with orthorhombic perovskite-type structure. Four platinum wires were wound around the sample to serve as current leads and potential probes. The sample was placed in the center of an alumina protection tube, through which a mixture of CO and CO_2 was allowed to flow. Electrical conductivity relaxation experiments were conducted as follows. After the sample was fully equilibrated in a selected atmosphere, a change in oxygen partial pressure (P_{O_2}) was imposed in an oxidizing or reducing direction by altering the mixing ratio of CO and CO_2, and then *dc* conductivity was recorded as a function of elapsed time until it reached a new stationary value. The P_{O_2} in the atmosphere was monitored by a zirconia sensor placed close to the sample. The experiments were performed at 900, 950, 1000, and 1050°C. The principle of the technique and more details of the experimental procedures were described in our previous reports (3, 4).

[1] To whom correspondence should be addressed.

0022-4596/95 $6.00

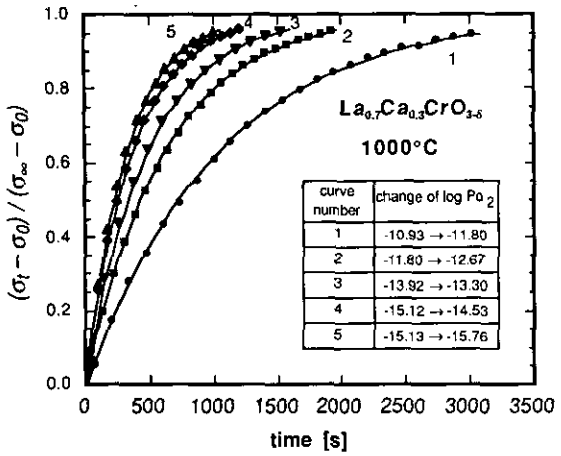

FIG. 1. Typical conductivity relaxation data of $La_{0.7}Ca_{0.3}CrO_{3-\delta}$ presented in the form of fractional conductivity change as a function of elapsed time. The solid curves were drawn by fitting the experimental data to Eq. [1].

3. RESULTS AND DISCUSSION

Figure 1 shows five sets of raw relaxation data for the composition of $x = 0.30$ at 1000°C in the form of fractional conductivity change as a function of elapsed time. The solid curves in the figure are drawn by nonlinear least-squares fitting of the measured data to the equation (see Ref. 4):

$$\frac{\sigma_{app}(t) - \sigma_{app}(0)}{\sigma_{app}(\infty) - \sigma_{app}(0)} = \quad [1]$$

$$1 - \sum_{n=1}^{\infty}\sum_{m=1}^{\infty} \frac{4L_c^2\exp(-\beta_n^2 D_{chem}t/a^2)}{\beta_n^2(\beta_n^2 + L_c^2)} \cdot \frac{2L_p^2\exp(-\gamma_m^2 D_{chem}t/l^2)}{\gamma_m^2(\gamma_m^2 + L_p^2 + L_p)},$$

where σ_{app} is the measured conductivity, D_{chem} is the chemical diffusion coefficient, t is diffusion time, and a and l are the radius and half-length of the sample, respectively. L_c and L_p are dimensionless parameters defined using the diffusion coefficient, D_{chem}, and the surface reaction rate constant, α, as

$$L_c = a\alpha/D_{chem} \quad [2]$$

$$L_p = l\alpha/D_{chem}, \quad [3]$$

which serve as a measure of the contribution of the surface reaction to the overall process. β_n and γ_m are respectively the nth and mth positive roots of the equations

$$\beta_n J_1(\beta_n) - L_c J_0(\beta_n) = 0 \quad [4]$$

$$\gamma_m \tan \gamma_m = L_p, \quad [5]$$

where J_0 and J_1 represent zeroth and first-order Bessel functions. The above equations are derived from the analytical solution of Fick's second law for a cylindrical geometry with consideration of the effect of surface reaction (4). Introduced for this derivation are the approximations that the surface reaction rate is linear with oxygen concentration at the surface, and that the carrier mobility is constant within each relaxation step with not too large a P_{O_2} change.

As can be clearly seen in Fig. 1, Eq. [1] fits very well to the experimental data. This suggests that the conductivity relaxation kinetics can be well described by a diffusion model with consideration of partial control by surface reaction. Looking through the series of relaxation curves, it is found that the relaxation kinetics becomes faster as the final P_{O_2} decreases. This means that larger chemical diffusion coefficients result as the final P_{O_2} decreases.

The chemical diffusion coefficient, in general, is closely related to the concentrations of moving defects in the material. This means that the defect equilibrium in the system of concern has to be made clear for discussing the P_{O_2} dependence of chemical diffusivity. The defect equilibrium in $La_{1-x}Ca_xCrO_{3-\delta}$ was discussed in our previous paper (5) on stationary electrical conductivity as a function of P_{O_2}, using a simple point defect model which is basically the same as those used to elucidate the defect equilibrium in Mg- and Sr-doped $LaCrO_3$ (6, 7). The point defect model is summarized as follows.

$La_{1-x}Ca_xCrO_{3-\delta}$ shows oxygen-deficient-type nonstoichiometry. The predominant point defects are Ca ions substituting on La-sites (Ca'_{La}) and double-positively charged oxygen vacancies ($V_O^{\cdot\cdot}$) with the electronic defects being holes (tetravalent Cr ions, $Cr_{Cr}^{\cdot}$). The symbols in parentheses are the Kröger–Vink notations for point defects (8) and will be used throughout this paper. The interaction between the defects and the surrounding atmosphere can be expressed as

$$O_O^{\times} + 2\,Cr_{Cr}^{\cdot} = \tfrac{1}{2}\,O_2 + V_O^{\cdot\cdot} + 2\,Cr_{Cr}^{\times} \quad [6]$$

and the equilibrium constant for this reaction is

$$K = \frac{[V_O^{\cdot\cdot}][Cr_{Cr}^{\times}]^2 P_{O_2}^{1/2}}{[O_O^{\times}][Cr_{Cr}^{\cdot}]^2}. \quad [7]$$

The following electroneutrality condition should be satisfied among the defect concentrations:

$$[Ca'_{La}] = [Cr_{Cr}^{\cdot}] + 2[V_O^{\cdot\cdot}]. \quad [8]$$

The above pseudochemical reaction indicates that the charge imbalance caused by the introduction of calcium

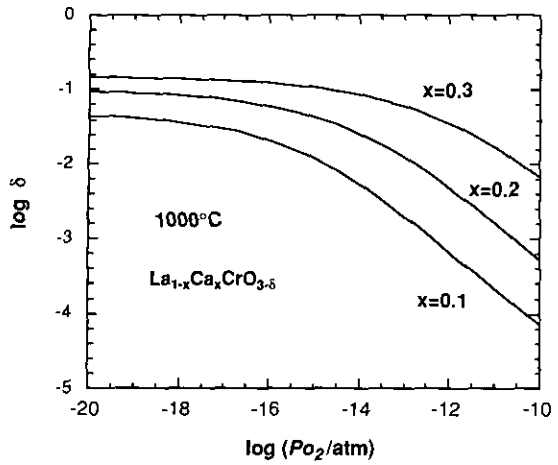

FIG. 2. Simulated oxygen nonstoichiometry of $La_{1-x}Ca_xCrO_{3-\delta}$ at 1000°C as a function of oxygen partial pressure.

is electronically compensated for by transforming part of the Cr^{3+} ions into a Cr^{4+} state at high P_{O_2}, while ionic compensation by the formation of oxygen vacancies becomes more significant as the P_{O_2} decreases.

Figures 2 and 3 show the effect of Ca-doping and temperature on the variation of oxygen vacancy concentration with P_{O_2} calculated by using the point defect model. The values of the equilibrium constant used in the calculation are listed in Table 1, which have been quoted from our previous paper (5). The vacancy concentration increases with a decrease in P_{O_2} in proportion to $P_{O_2}^{-1/2}$ at high P_{O_2} and it asymptotically approaches the limiting value determined by the level of Ca-doping. At a given P_{O_2}, the higher vacancy concentration is expected for the higher Ca-doping and higher temperatures.

In the conductivity relaxation experiments, the chemical diffusion coefficient can be obtained as a function of the final P_{O_2} of each relaxation run. As has been pointed out, however, the variation in chemical diffusivity is to be examined in relation to the change in defect concentration rather than to the P_{O_2} change. The oxygen vacancy concentration corresponding to the final P_{O_2} of each relaxation run has been calculated using the point defect model, and its relation to the measured chemical diffusion coefficient is presented in Figs. 4 and 5. Open and closed symbols represent the results from reduction and oxidation runs, respectively. The figures clearly show that D_{chem} increases with an increase in oxygen vacancy concentration, suggesting that chemical diffusion proceeds via an oxygen vacancy diffusion mechanism.

In the process of conductivity relaxation, the sample surface first reaches equilibrium with a new atmosphere, which generates a concentration gradient of oxygen vacancies within the sample. This is a driving force of oxygen movement. The electroneutrality condition (Eq. [8]) requires a simultaneous setup of a concentration gradient

TABLE 1
Equilibrium Constant of the Defect Reaction [6]

x	Temperature (°C)	K_{ox} ($atm^{1/2}$)
0.1	1000	1.88×10^{-8}
0.2	1000	2.89×10^{-8}
0.3	900	1.48×10^{-8}
0.3	950	4.61×10^{-8}
0.3	1000	1.37×10^{-7}
0.3	1050	2.99×10^{-7}

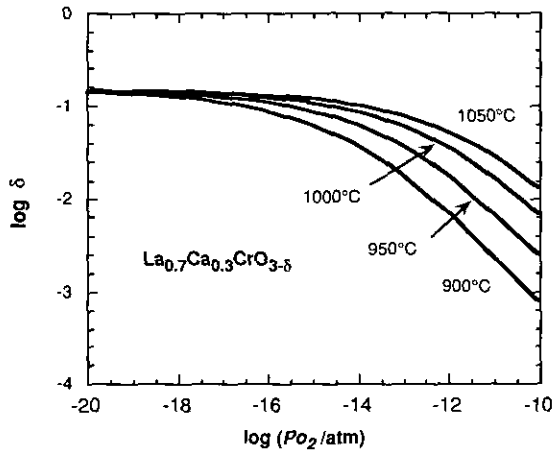

FIG. 3. Simulated oxygen nonstoichiometry of $La_{0.7}Ca_{0.3}CrO_{3-\delta}$ as a function of oxygen partial pressure at 900, 950, 1000, and 1050°C.

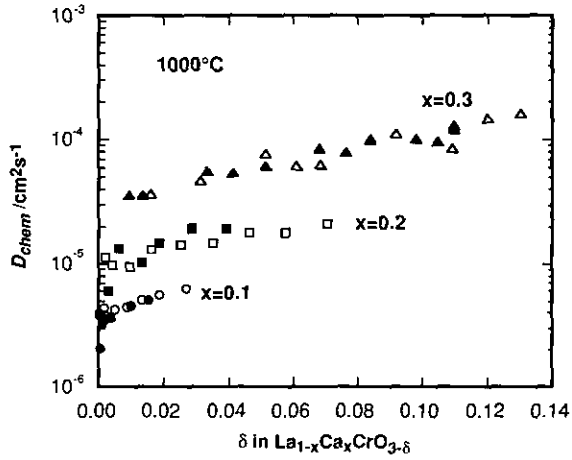

FIG. 4. Relationship between chemical diffusion coefficient and oxygen vacancy concentration in $La_{1-x}Ca_xCrO_{3-\delta}$ at 1000°C. Open and closed symbols are for the results from reduction and oxidation runs, respectively.

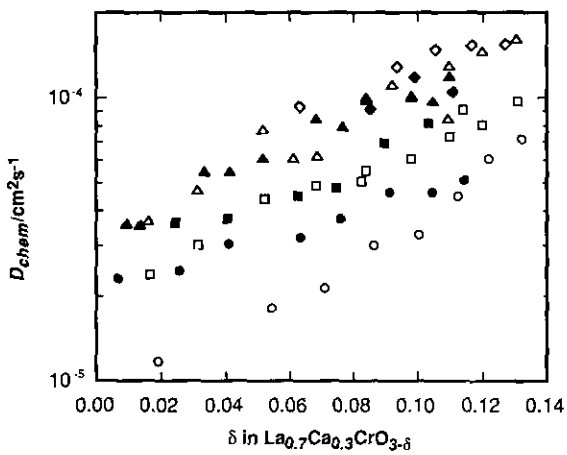

FIG. 5. Relationship between chemical diffusion coefficient and oxygen vacancy concentration in $La_{0.7}Ca_{0.3}CrO_{3-\delta}$ at 900° (○, ●), 950° (□, ■), 1000° (△, ▲), and 1050°C (◇, ◆). Open and closed symbols are for the results from reduction and oxidation runs, respectively.

of electron holes in the opposite direction, which forces the electron holes to counterdiffuse with the oxygen vacancies. The moving species in the chemical diffusion process are thus oxygen vacancies and electron holes. For a quantitative treatment of simultaneous motions of charged species, Wagner's theory on oxidation of metals (9–11) and the ambipolar diffusion theory (12) are known. Assuming that the net current along the diffusional direction is zero (the so-called "coupled current condition") and that the electronic transference number can be approximated as unity, Wagner's theory and the ambipolar diffusion theory, respectively, formulate the chemical diffusion coefficient as

$$D_{chem} = -\tfrac{1}{2}D_v \frac{\partial \ln P_{O_2}}{\partial \ln [V_O^{\cdot\cdot}]} \qquad [9]$$

and

$$\begin{aligned} D_{chem} &= \frac{D_h D_V (4[V_O^{\cdot\cdot}] + p)}{4[V_O^{\cdot\cdot}]D_V + pD_h} \\ &= t_h D_V + t_i D_h \\ &= D_V \left(1 + \frac{4[V_O^{\cdot\cdot}]}{p}\right), \end{aligned} \qquad [10]$$

where D_V and D_h are the diffusion coefficients of oxygen vacancies and electron holes, t_i and t_h are ionic and electronic transference numbers, and p denotes the hole concentration. The vacancy diffusion coefficient, D_V, can be considered constant when the interaction between defects is negligibly small (the approximation of the dilute solution). Setting the D_V as a point of reference, the enhancement factor (e.f.) of D_{chem} is defined as

$$\text{ef} = D_{chem}/D_V. \qquad [11]$$

Using Eqs. [9] and [10] into Eq. [11], we get the e.f. as a function of defect concentration and oxygen partial pressure:

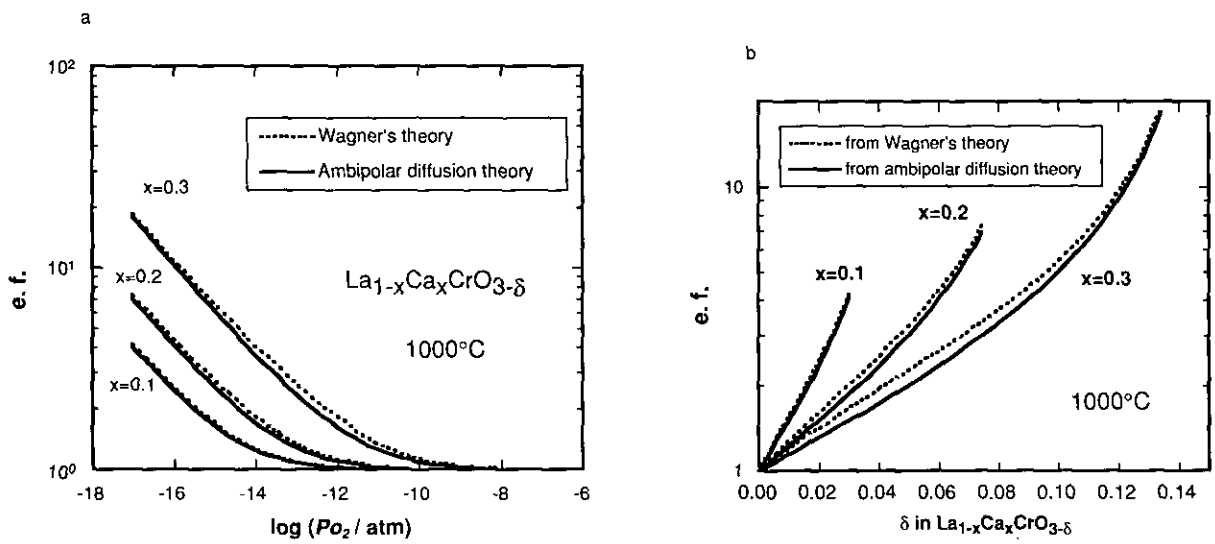

FIG. 6. Calculated enhancement factor of $La_{1-x}Ca_xCrO_{3-\delta}$ at 1000°C as a function of (a) oxygen partial pressure and (b) oxygen vacancy concentration.

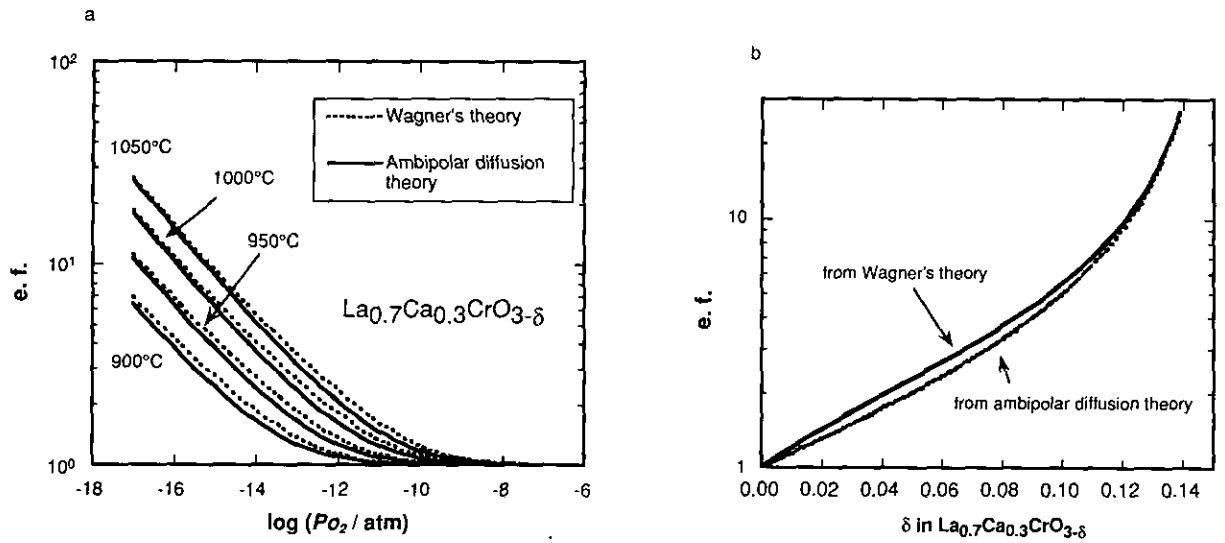

FIG. 7. Calculated enhancement factor of $La_{0.7}Ca_{0.3}CrO_{3-\delta}$ at four different temperatures as a function of (a) oxygen partial pressure and (b) oxygen vacancy concentration.

$$\text{ef} = -\tfrac{1}{2}\frac{\partial \ln P_{O_2}}{\partial \ln [V_O^{\cdot\cdot}]} \qquad [12]$$

and

$$\text{ef} = 1 + \frac{4[V_O^{\cdot\cdot}]}{p}, \qquad [13]$$

for the Wagner's treatment and the ambipolar diffusion treatment, respectively. These values can be estimated when the defect concentrations are available as a function of P_{O_2}. The defect concentrations calculated by using the equilibrium constants in Table 1 into Eq. [7] are substituted for the corresponding parameters in the above equations to give the e.f. Figs. 6a and 7a show the P_{O_2} dependence, and Figs. 6b and 7b show the relationships with the vacancy concentration. In Fig. 7b, no distinct differences can be observed in the results for the four different temperatures; four curves seem to merge into a single curve. It can be seen that the e.f. asymptotically approaches unity as the P_{O_2} increases. This means that at relatively high P_{O_2}, D_{chem} is equal to D_V and does not depend on P_{O_2}. On the other hand, the e.f. increases as the P_{O_2} decreases or the vacancy concentration increases. This predicts that D_{chem} is an increasing function of oxygen vacancy concentration, which agrees well with the experi-

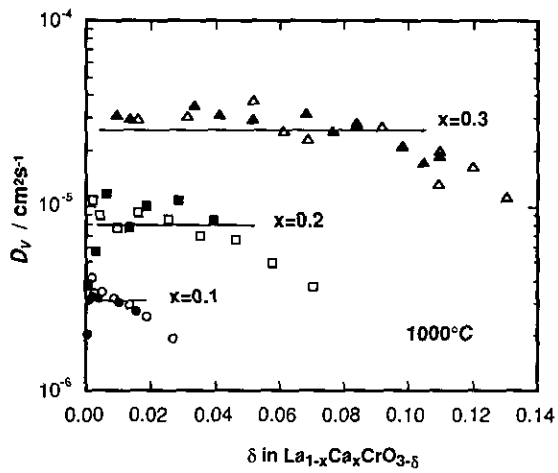

FIG. 8. Oxygen vacancy diffusion coefficient of $La_{1-x}Ca_xCrO_{3-\delta}$ at 1000°C. Open and closed symbols are for the results from reduction and oxidation runs, respectively.

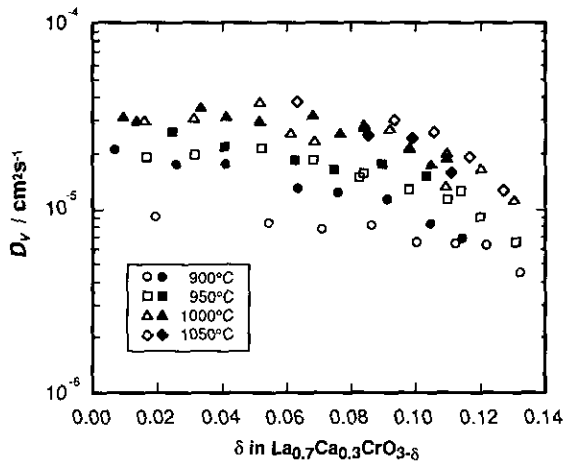

FIG. 9. Oxygen vacancy diffusion coefficient of $La_{0.7}Ca_{0.3}CrO_{3-\delta}$ at 900°, 950, 1000, and 1050°C. Open and closed symbols are for the results from reduction and oxidation runs, respectively.

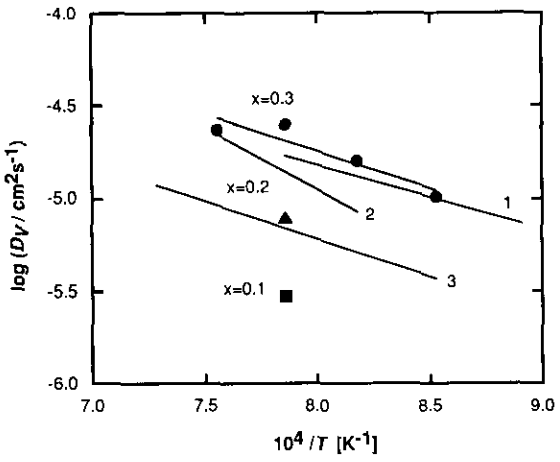

FIG. 10. Temperature dependence of oxygen vacancy diffusion coefficient of $La_{1-x}Ca_xCrO_{3-\delta}$; ■, $x = 0.1$; ▲, $x = 0.2$; and ●, $x = 0.3$. The data of 1: $LaCoO_{3-\delta}$, 2: $La_{0.75}Sr_{0.25}FeO_{3-\delta}$, and 3: $La_{0.9}Sr_{0.1}FeO_{3-\delta}$ are taken from Ref. (12).

mental results shown in Figs. 4 and 5. Higher temperatures and increased Ca-doping have the effect of increasing e.f. at a given P_{O_2} and oxygen vacancy concentration.

The two theories introduced for discussing the enhancement of D_{chem} have provided very similar results. For further analyses, the e.f. calculated by using the ambipolar diffusion theory will be used, because this treatment is more general than the other in that it requires no assumptions of local equilibrium (13). Figures 8 and 9 plot the D_V converted from the measured D_{chem} by using the calculated e.f. into Eq. [13]. Figure 8 clearly shows that D_V is constant at low oxygen vacancy concentrations, suggesting that the oxygen vacancies are not interacting. However, at relatively high vacancy concentrations, there is a trend for D_V to decrease, which implies a reduced mobility of oxygen vacancies resulting from interactions between defects. The same trends can be observed in Fig. 9, although they are difficult to distinguish because of the number of data points.

The average of D_V in the region of its insignificant dependence on vacancy concentration is taken as a representative value for a particular condition: Ca-doping level and temperature. Figure 10 shows the temperature dependence of D_V thus determined as compared with that of typical mixed-conducting perovskites based on $LaFeO_3$ and $LaCoO_3$ (14). The D_V of Ca-doped $LaCrO_3$ obtained in the present study is similar to that of other perovskite-type oxides, both in magnitude and in activation energy.

4. CONCLUSION

The chemical diffusion coefficient of polycrystalline Ca-doped $LaCrO_3$ measured by the electrical conductivity relaxation method was found to increase with increasing oxygen vacancy concentration. This suggests that in the process of chemical diffusion, oxygen is transported through lattice diffusion of oxide ions by the vacancy diffusion mechanism. The dependence of chemical diffusivity on the vacancy concentration was theoretically elucidated by combining the Wagner's theory or the ambipolar diffusion theory with the point defect model. The enhancement factor of the chemical diffusion coefficient calculated by using the ambipolar diffusion theory allowed us to derive the vacancy diffusion coefficient. The constancy of the vacancy diffusion coefficient obtained at low vacancy concentrations suggests that the vacancies are not interacting. Ca-doped $LaCrO_3$ exhibits a vacancy diffusion coefficient comparable to that of Fe- or Co-based perovskites whose fast oxygen diffusion has been experimentally demonstrated in the literature.

REFERENCES

1. C. J. Yu, D. M. Sparlin, and H. U. Anderson, *J. Am. Ceram. Soc.* **70,** C189 (1987).
2. V. E. J. van Dieten, J. P. Dekker, and J. Schoonman, *in* "Proceedings, First International Symposium on Ionic and Mixed Conducting Ceramics," Phoenix, Oct. 1991 (T. A. Ramanarayanan and H. L. Tuller, Ed.), PV 91-12, The Electrochemical Society Proceedings Series, Pennington, NJ, p. 216.
3. I. Yasuda and T. Hikita, *in* "Proceedings, Second International Symposium on Solid Oxide Fuel Cells," Athens, July 1991 (F. Grosz, P. Zegers, S. C. Singhal, and O. Yamamoto, Eds.), Report EUR 13564 EN, Commission of The European Communities, p. 645.
4. I. Yasuda and T. Hikita, *J. Electrochem. Soc.* **141,** 1268 (1994).
5. I. Yasuda and T. Hikita, *J. Electrochem. Soc.* **140,** 1699 (1993).
6. B. K. Flandermeyer, M. M. Nasrallah, A. K. Agarwal, and H. U. Anderson, *J. Am. Ceram. Soc.* **67,** 195 (1984).
7. J. Mizusaki, S. Yamauchi, K. Fueki, and A. Ishikawa, *Solid State Ionics* **12,** 119 (1984).
8. F. A. Kröger, *in* "The Chemistry of Imperfect Crystals." North-Holland, Amsterdam, 1964.
9. C. Wagner, *Z. Phys. Chem. B* **11,** 139 (1930).
10. C. Wagner, *Z. Phys. Chem. B* **21,** 25 (1933).
11. C. Wagner, *Z. Phys. Chem. B* **32,** 447 (1936).
12. W. van Roosbroeck, *Phys. Rev.* **91,** 282 (1953).
13. L. Heye, *in* "Solid Electrolytes (Topics in Applied Physics, Vol. 21)" (S. Geller, Ed.), p. 199. Springer-Verlag, New York/Berlin, 1977.
14. T. Ishigaki, S. Yamauchi, K. Kishio, J. Mizusaki, and K. Fueki, *J. Solid State Chem.* **73,** 179 (1988).